

# Articles

## Synthesis and Characterization of Blue-Light-Emitting Alternating Copolymers of 9,9-Dihexylfluorene and 9-Arylcarbazole

Wai-Yeung Wong,<sup>\*,†</sup> Li Liu,<sup>†,‡</sup> Dongmui Cui,<sup>†</sup> Louis M. Leung,<sup>†</sup> Chin-Fai Kwong,<sup>†</sup> Tik-Ho Lee,<sup>†</sup> and Ho-Fung Ng<sup>†</sup>

Department of Chemistry and Centre for Advanced Luminescence Materials, Hong Kong Baptist University, Waterloo Road, Kowloon Tong, Hong Kong, P.R. China, and Faculty of Chemistry and Material Science, Hubei University, Wuhan 430062, P.R. China

Received April 4, 2005; Revised Manuscript Received April 25, 2005

**ABSTRACT:** Several soluble and well-defined copolymers of 9,9-dihexyl-2,7-fluorene and 9-aryl-3,6-carbazole (aryl = phenyl, *p*-methylphenyl, *p*-methoxyphenyl) were prepared in good yields by Suzuki-type coupling polymerization of fluorene–diboronic ester with some 9-aryl-3,6-dibromocarbazole derivatives. These copolymers showed high glass transition temperatures, and their regiochemical structures and physical properties were studied by gel permeation chromatography, NMR, UV absorption, elemental analysis, thermogravimetry, photoluminescence, and quantum yield measurements. The influence of the carbazole core and its aryl substituent on the photophysical, electrochemical, and electroluminescent properties of these alternating fluorene/carbazole copolymers has been investigated. Both the absorption and photoluminescence peaks of these copolymers are blue-shifted relative to the poly(9,9-dihexylfluorene) homopolymer (**PF-C<sub>6</sub>**), and cyclic voltammetry showed that these copolymers have their HOMO energy levels raised relative to that of **PF-C<sub>6</sub>**, thus facilitating hole injection into the copolymers from the indium tin oxide (ITO) anode. The copolymers exhibited very good thermal stability and blue emission in both solution and the solid state. Unlike **PF-C<sub>6</sub>**, these copolymers showed high photoluminescent stability toward annealing action under vacuum. Blue electroluminescence with negligible low-energy emission bands was successfully achieved from these copolymers by using bathocuproine (BCP) as a hole-blocking layer and aluminum tris(8-hydroxyquinoline) (Alq<sub>3</sub>) as an electron-injection/transporting layer.

### Introduction

Since the pioneer work by the Cambridge researchers,<sup>1</sup> organic polymeric compounds have emerged as a new class of electroluminescent materials in organic light-emitting diodes (OLEDs) technology which are important for the next generation of flat panel displays.<sup>2</sup> Polymer LEDs (PLEDs) based on conjugated polymers with different chemical structures emitting different colors across the entire visible spectrum have been fabricated.<sup>2,3</sup> Along these lines of research in both academia and industry, there is still a great demand to develop blue-light-emitting polymers on the path toward full-color polymer displays. They can be used either as the active layer in PLEDs or as the host material for internal color conversion techniques.<sup>4</sup> While a stable blue PLED is still a challenge for polymer scientists, it is hard to achieve a balanced charge injection because of the large band gap between the HOMO and LUMO energy levels.<sup>5</sup> In this regard, a number of research reports have highlighted the design and investigations of carbazole- and fluorene-containing polymers or small molecules.<sup>6</sup> Carbazole is a well-known hole-transporting (HT) unit due to the electron-donating capabilities

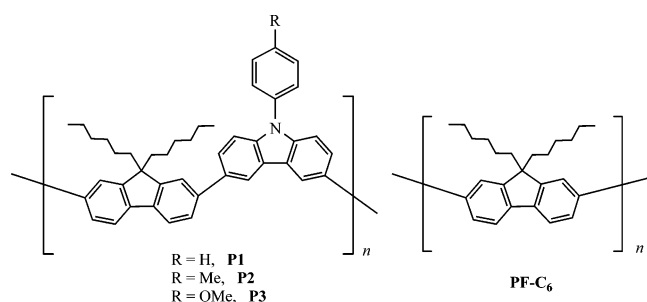
associated with its nitrogen atom.<sup>7</sup> In the past decade, homopolymers and copolymers of fluorene were shown to be a very important class of blue-emitting materials for use in PLEDs due to their thermal and chemical stability and their high efficient blue emission in both photoluminescence (PL) and electroluminescence (EL).<sup>6,8</sup> Fluorenes contain a rigid planar biphenyl unit and substituent derivatization at the C-9 position of the monomeric fluorenes offers the prospect of controlling polymer properties such as solubility, emission wavelengths, processability, and potential interchain interactions in films.<sup>9</sup> However, the main drawbacks attributed to many of these systems are aggregation and/or excimers formation in the solid state,<sup>10</sup> their intractability, insufficient stability, and solubility, and high-energy barrier for hole injection (e.g., HOMO of poly(9,9-dihexylfluorene) homopolymer  $\approx -5.5$  eV).<sup>11</sup> Recent findings also indicated that keto defects in the polymer backbone, arising from photo- and/or electrooxidative degradation of 9,9-dialkylated poly(2,7-fluorene)s (PFs), were mainly responsible for this strong low-energy emission.<sup>12</sup> To circumvent these obstacles, a number of elegant synthetic methods have been developed to make new PF derivatives, and many approaches to stabilize the pure blue emission from PFs have also been explored with varying degrees of success. This includes the use of bulky substituents and end-capping groups in the main chain<sup>13</sup> and the deliberate inclusion of conjugation-

<sup>†</sup> Hong Kong Baptist University.

<sup>‡</sup> Hubei University.

\*Corresponding author: Fax +852-3411-7348; e-mail rwywong@hkbu.edu.hk.

Chart 1



interrupting groups in PFs.<sup>14</sup> The decreased aggregation phenomena in PFs by introducing disordered 9-ethylcarbazole comonomer units in the resulting copolymers via the Ni-catalyzed Yamamoto coupling reaction can also improve the luminescent stability by limiting the intrinsic conjugation length in the polymer backbone.<sup>15</sup> One intriguing approach to address the deficiency in hole injection is based on the modification of chemical structures of PFs by adding electron-donating moieties, such as thiophene,<sup>16</sup> triphenylamine,<sup>17</sup> and carbazole,<sup>18</sup> into the p-type PF backbone. It was also well-documented that 9-substituted carbazole molecules and their derivatives are useful HT chromophores for small-molecule OLEDs nowadays.<sup>19</sup>

In the present study, we prepared a new series of thermally stable alternating 9,9-dihexylfluorene/9-arylcarbazole hybrid copolymers (aryl = C<sub>6</sub>H<sub>4</sub>-R, R = H **P1**, Me **P2**, OMe **P3**) with well-defined chemical structures (Chart 1) and examined the effects of the functionalized carbazole content on the photophysical, redox, and electroluminescent properties of the resulting kinked copolymers. The purpose of this study was to incorporate the electron-rich 9-arylcarbazole HT groups into the PF main chain to raise the HOMO level, while retaining their emission color in the blue region. Presumably, the use of the more robust 9-aryl groups in the present system should have the added advantage of increasing the thermal stability and glass transition temperature of the resulting copolymers as compared to their 9-alkyl-substituted congeners.

## Experimental Section

**General.** All reactions were carried out under a nitrogen atmosphere with the use of standard Schlenk techniques, but no special precautions were taken to exclude oxygen during workup. Solvents were predried and distilled from appropriate drying agents. All reagents and chemicals, unless otherwise stated, were purchased from commercial sources and used without further purification. Preparative TLC was performed on 0.7 mm silica plates (Merck Kieselgel 60 GF<sub>254</sub>) prepared in our laboratory. The compound 9,9-dihexylfluorene-2,7-bis(trimethylene boronate) was prepared by the literature method.<sup>11,20</sup> Infrared spectra were recorded as CH<sub>2</sub>Cl<sub>2</sub> solutions using a Perkin-Elmer Paragon 1000 PC or Nicolet Magna 550 series II FTIR spectrometer. NMR spectra were measured in appropriate solvents on a JEOL EX270 or a Varian Inova 400 MHz FT-NMR spectrometer, with <sup>1</sup>H and <sup>13</sup>C NMR chemical shifts quoted relative to TMS. Fast atom bombardment (FAB) and electron impact (EI) mass spectra were recorded on a Finnigan MAT SSQ710 mass spectrometer. Electronic absorption spectra were obtained with a HP 8453 UV-vis spectrometer. For solid-state emission spectral measurements, the 325 nm line of a He-Cd laser was used as an excitation source. The luminescence spectra were analyzed by a 0.25 m focal length double monochromator with a Peltier cooled photomultiplier tube and processed with a lock-in-amplifier. The solution emission spectra were measured on a PTI Fluorescence

Master Series QM1 spectrophotometer. The fluorescence quantum yields ( $\Phi_{\text{F}}$ ) were determined in CHCl<sub>3</sub> solutions (ca. 10<sup>-5</sup> M based on  $M_{\text{w}}$ ) at 293 K against the quinine sulfate (0.1 N H<sub>2</sub>SO<sub>4</sub>) standard ( $\Phi_{\text{F}} = 0.54$ ). Cyclic voltammetry experiments were done with a Princeton Applied Research (PAR) model 273A potentiostat. A conventional three-electrode configuration consisting of a glassy-carbon working electrode, a Pt-wire counter electrode, and an Ag/AgCl reference electrode was used. The solvents in all measurements were deoxygenated CH<sub>2</sub>Cl<sub>2</sub> or THF, and the supporting electrolyte was 0.1 M [Bu<sub>4</sub>N]PF<sub>6</sub>. Ferrocene was added as a calibrant after each set of measurements, and all potentials reported were quoted with reference to the ferrocene-ferrocenium couple at a scan rate of 100 mV/s. The molecular weights of the polymers were determined by gel permeation chromatography (GPC) on a HP 1050 series HPLC with visible wavelength and fluorescent detectors and were calibrated against polystyrene standards. Thermal analyses were performed with Perkin-Elmer Pyris Diamond DSC and Perkin-Elmer DTA-7 thermal analyzers at a heating rate of 20 °C/min.

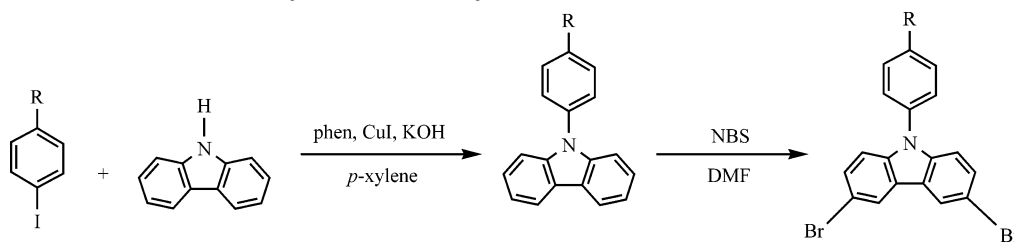
**PLED Fabrication and Measurements.** Before device fabrication, the ITO-coated glass substrates were cleaned by ultrasonic baths in organic solvents followed by ozone treatment. The multilayer devices were assembled in the following sequence: indium tin oxide (ITO) with sheet resistance of 80 Ω/sq on glass substrate (anode), 90 nm of each of the light-emitting copolymers **P1–P3**, 25 nm of bathocuproine (BCP), 20 nm of aluminum tris(8-hydroxyquinoline) (Alq<sub>3</sub>), and 80 nm of Ag (cathode). A thin layer of the polymer was spin-coated onto the ITO substrate from its CHCl<sub>3</sub> solution. The organic and electrode layers were deposited at a rate of 1 and 10 Å/s, respectively, under a pressure of 4 × 10<sup>-6</sup> Torr without breaking vacuum between each vacuum deposition process. The thickness of each layer was measured in situ by a quartz crystal sensor and ex situ by a stylus profilometer (Tencor α-step 500). The devices were tested in air under ambient conditions with no protective encapsulation. The EL spectra were measured by a Larry 2048L CCD system and current-voltage-luminance characteristics were recorded in air with a Keithley 236 source measuring unit and International Light Corp. (model ILC1400) light meter.

**3,6-Dibromo-9-phenylcarbazole.** A mixture of 9-phenylcarbazole (126.7 mg, 0.52 mmol, from Aldrich) and *N*-bromosuccinimide (NBS, 213.2 mg, 1.20 mmol) was stirred in dimethylformamide (50 mL) at 0 °C for 3 h. Ice was then added to the mixture, and a white precipitate appeared. After filtration and drying, a white solid was obtained. Further purification can be accomplished by recrystallization from a toluene/hexane solvent mixture, and the product was isolated in 80% yield (166.8 mg). <sup>1</sup>H NMR (CDCl<sub>3</sub>): δ (ppm) 8.20 (m, 2H, Ar), 7.64–7.59 (m, 2H, Ar), 7.52–7.48 (m, 5H, Ar), 7.27–7.24 (m, 2H, Ar). <sup>13</sup>C NMR (CDCl<sub>3</sub>): δ (ppm) 139.72, 136.64, 130.00, 129.25, 127.99, 126.84, 123.81, 123.10, 112.95, 111.42 (Ar). FAB-MS (*m/z*): 401 [M<sup>+</sup>]. Anal. Calcd for C<sub>18</sub>H<sub>11</sub>NBr<sub>2</sub>: C, 53.90; H, 2.76; N, 3.49. Found: C, 53.78; H, 2.55; N, 3.20.

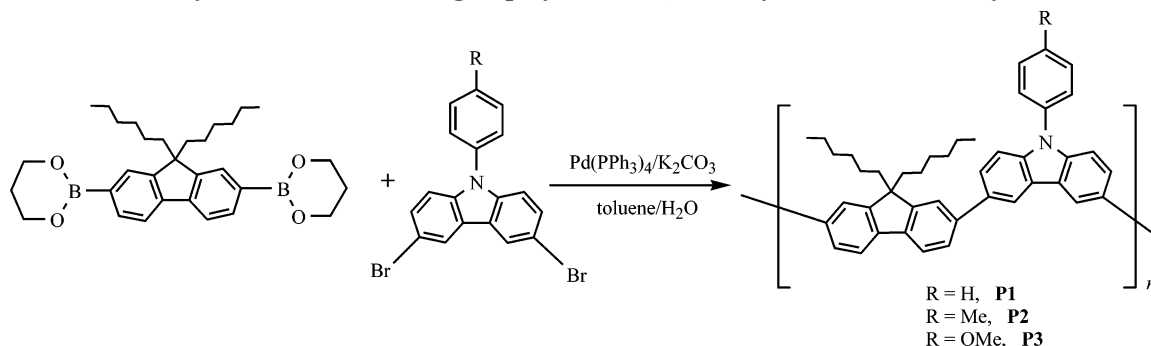
**3,6-Dibromo-9-(*p*-methylphenyl)carbazole.** To a chilled solution of 9-(*p*-methylphenyl)carbazole (121.6 mg, 0.47 mmol) in DMF (30 mL) at 0 °C, NBS (193.4 mg, 1.09 mmol) was added dropwise. The mixture was stirred for 3 h at room temperature. Ice was added to the mixture to give a white precipitate. After filtration and drying, a white solid was obtained which was recrystallized from toluene/hexane to afford a pure sample of the title compound in 78% yield (153.0 mg). <sup>1</sup>H NMR (CDCl<sub>3</sub>): δ (ppm) 8.16 (m, 2H, Ar), 7.48–7.45 (m, 2H, Ar), 7.40–7.31 (m, 4H, Ar), 7.24–7.18 (m, 2H, Ar), 2.47 (s, 3H, Me). <sup>13</sup>C NMR (CDCl<sub>3</sub>): δ (ppm) 139.87, 137.99, 133.92, 130.55, 129.16, 126.65, 123.68, 123.03, 112.77, 111.42 (Ar), 21.32 (Me). FAB-MS (*m/z*): 415 [M<sup>+</sup>]. Anal. Calcd for C<sub>19</sub>H<sub>13</sub>NBr<sub>2</sub>: C, 54.97; H, 3.16; N, 3.37. Found: C, 54.79; H, 3.02; N, 3.15.

**3,6-Dibromo-9-(*p*-methoxyphenyl)carbazole.** This compound was prepared using the same conditions as described above, but 9-(*p*-methoxyphenyl)carbazole was used instead to produce a white solid in 94% yield. <sup>1</sup>H NMR (CDCl<sub>3</sub>): δ (ppm) 8.19 (m, 2H, Ar), 7.51–7.47 (m, 2H, Ar), 7.40–7.37 (m, 2H, Ar), 7.19–7.09 (m, 4H, Ar), 3.92 (s, 3H, OMe). <sup>13</sup>C NMR

Scheme 1. Synthesis of 9-Aryl-3,6-dibromocarbazole Monomers



Scheme 2. Synthesis of Alternating Copolymers of 9,9-Dihexylfluorene and 9-Arylcarbazole



(CDCl<sub>3</sub>):  $\delta$  (ppm) 159.04, 140.09, 129.12, 129.06, 128.18, 123.49, 122.98, 115.12, 112.67, 111.30 (Ar), 55.62 (OMe). FAB-MS ( $m/z$ ): 431 [M<sup>+</sup>]. Anal. Calcd for C<sub>19</sub>H<sub>13</sub>NBr<sub>2</sub>O: C, 52.93; H, 3.04; N, 3.25. Found: C, 52.74; H, 2.98; N, 3.08.

**Polymerization.** General Procedure of Polymerization through the Suzuki Coupling Reaction. To a mixture of 9,9-dihexylfluorene-2,7-bis(trimethylene boronate) (1 equiv), dibromocarbazole derivative (1 equiv), and Pd(PPh<sub>3</sub>)<sub>4</sub> (1.0 mol %) was added a mixture of toluene and 2 M K<sub>2</sub>CO<sub>3</sub>(aq) (3:2, v/v). The mixture was vigorously stirred at 85–90 °C for 48 h under the protection of nitrogen. After the mixture was cooled to room temperature, it was poured into a stirred mixture of MeOH and deionized water (10:1, v/v). The dull white solid precipitated was obtained by filtration, and it was subsequently washed with MeOH and water followed by MeOH again. The polymer was further purified by washing with acetone in a Soxhlet apparatus for 24 h to remove oligomers and catalyst residues and was dried under reduced pressure. Yields: 66–78%.

Data for **P1**: white solid (yield: 66%). <sup>1</sup>H NMR (CDCl<sub>3</sub>):  $\delta$  (ppm) 8.54 (m, 2H, Ar), 7.83–7.53 (m, 13H, Ar), 7.23 (m, 2H, Ar), 2.13 (m, 4H, CCH<sub>2</sub>), 1.11 (m, 12H, (CH<sub>2</sub>)<sub>3</sub>), 0.78 (m, 10H, CH<sub>2</sub>CH<sub>3</sub>). <sup>13</sup>C NMR (CDCl<sub>3</sub>):  $\delta$  (ppm) 151.73, 140.77, 140.67, 139.63, 137.68, 134.25, 130.05, 130.00, 127.00, 126.22, 125.84, 124.11, 121.69, 119.95, 118.89, 110.18 (Ar), 55.35 (quat C), 40.57, 31.48, 29.73, 23.83, 22.58, 14.07 (C<sub>6</sub>H<sub>13</sub>). Anal. Calcd for (C<sub>43</sub>H<sub>43</sub>N)<sub>n</sub>: C, 90.01; H, 7.55; N, 2.44. Found: C, 89.79; H, 7.35; N, 2.20.

Data for **P2**: white solid (yield: 78%). <sup>1</sup>H NMR (CDCl<sub>3</sub>):  $\delta$  (ppm) 8.54 (m, 2H, Ar), 7.84–7.72 (m, 8H, Ar), 7.53–7.47 (m, 6H, Ar), 2.53 (s, 3H, Me), 2.14 (m, 4H, CCH<sub>2</sub>), 1.11 (m, 12H, (CH<sub>2</sub>)<sub>3</sub>), 0.78 (m, 10H, CH<sub>2</sub>CH<sub>3</sub>). <sup>13</sup>C NMR (CDCl<sub>3</sub>):  $\delta$  (ppm) 151.73, 140.93, 140.71, 139.61, 137.52, 134.97, 134.08, 130.57, 126.84, 126.20, 125.81, 124.00, 121.69, 119.93, 118.85, 110.18 (Ar), 55.34 (quat C), 40.57, 31.48, 29.72, 23.82, 22.57, 14.07 (C<sub>6</sub>H<sub>13</sub>), 21.27 (Me). Anal. Calcd for (C<sub>44</sub>H<sub>45</sub>N)<sub>n</sub>: C, 89.90; H, 7.72; N, 2.38. Found: C, 89.68; H, 7.45; N, 2.15.

Data for **P3**: white solid (yield: 75%). <sup>1</sup>H NMR (CDCl<sub>3</sub>):  $\delta$  (ppm) 8.53 (m, 2H, Ar), 7.83–7.72 (m, 8H, Ar), 7.56–7.44 (m, 4H, Ar), 7.22–7.16 (m, 2H, Ar), 3.95 (s, 3H, OMe), 2.14 (m, 4H, CCH<sub>2</sub>), 1.11 (m, 12H, (CH<sub>2</sub>)<sub>3</sub>), 0.77 (m, 10H, CH<sub>2</sub>CH<sub>3</sub>). <sup>13</sup>C NMR (CDCl<sub>3</sub>):  $\delta$  (ppm) 158.81, 150.75, 141.16, 140.63, 140.29, 139.50, 133.94, 130.17, 128.37, 126.14, 125.95, 123.81, 121.63, 119.73, 115.04, 110.05 (Ar), 55.62 (OMe), 55.39 (quat C), 40.63, 31.57, 29.81, 23.95, 22.67, 14.18 (C<sub>6</sub>H<sub>13</sub>). Anal. Calcd for (C<sub>44</sub>H<sub>45</sub>NO)<sub>n</sub>: C, 87.52; H, 7.51; N, 2.32. Found: C, 87.34; H, 7.38; N, 2.12.

## Results and Discussion

**Synthesis and Characterization.** The general synthetic routes for the monomer synthesis and polymerization are outlined in Schemes 1 and 2, respectively. First, the N-arylation of carbazole was carried out by the modified Ullmann condensation between carbazole and the corresponding *p*-iodoarene under the CuI/phen/KOH catalytic system.<sup>21</sup> NBS was used to brominate the 3,6-position of 9-arylcarbazole derivatives with high yields to furnish the dibromocarbazole comonomers. A complementary synthetic route can also be utilized for the preparation of 9-aryl-3,6-dibromocarbazole in a similar yield by condensing the commercially available 3,6-dibromocarbazole with the appropriate *p*-iodoarene. The synthesis of a new series of fluorene-based hybrid conjugated polymers **P1–P3** comprised of alternating 9,9-dihexyl-2,7-fluorene and 9-aryl-3,6-carbazole depicted in Scheme 2 is based on the palladium-catalyzed Suzuki coupling reaction, which was carried out in a mixture (3:2 in volume) of toluene and aqueous K<sub>2</sub>CO<sub>3</sub> solution containing 1 mol % Pd(PPh<sub>3</sub>)<sub>4</sub> under vigorous stirring at 85–90 °C for 48 h in the nitrogen atmosphere.<sup>11</sup> The feed mole ratios of the reacting monomers were 1:1 for the polymer synthesis to give alternating copolymers containing both of the components. The obtained polymers were further purified by washing with acetone in a Soxhlet apparatus for 24 h to remove oligomers and catalyst residues and were dried under reduced pressure at room temperature. After purification and drying, the polymers **P1–P3** were obtained as white fibrous solids in overall good yields. All the new polymers are air-stable and can be stored without any special precautions. They generally exhibit good solubility in chlorocarbons such as CH<sub>2</sub>Cl<sub>2</sub> and CHCl<sub>3</sub> but are insoluble in aliphatic hydrocarbons. We found that these copolymers can cast tough, free-standing thin films of good quality from appropriate solvents for optical characterization. The chemical structures of the polymers were verified by <sup>1</sup>H and <sup>13</sup>C NMR spectroscopy and elemental analysis. Since the proton resonance of the polymers is broadened, the coupling constants could not be obtained accurately. In the proton NMR spectrum



**Table 1. Structural and Thermal Properties of Copolymers P1–P3**

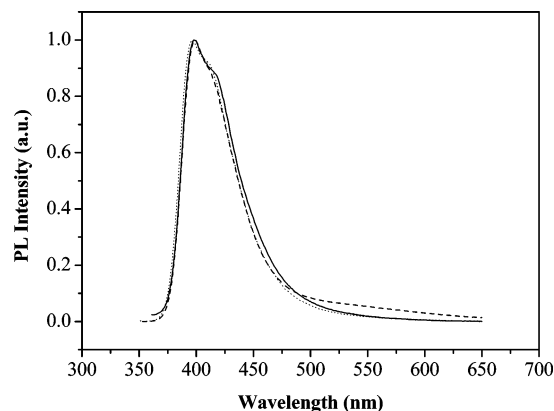
polymer	$M_n$	$M_w$	$M_w/M_n$	DP <sup>a</sup>	$T_d(\text{onset})$ (°C)	$T_g$ (°C)
<b>P1</b>	5800	7520	1.3	13	440	170
<b>P2</b>	8140	12000	1.5	21	446	155
<b>P3</b>	5720	7500	1.3	13	412	174

<sup>a</sup> DP = degree of polymerization.

of each polymer, there are three clear single broad peaks in the aliphatic region, which correspond to the dihexyl chains. The protons of the fluorene and carbazole rings can be assigned in the aromatic region. The characteristic peak at around  $\delta$  2.53 ppm is due to the methyl proton in **P2** whereas the singlet at  $\delta$  3.95 is assigned to the three protons of the methoxy group in **P3**. In fact, the  $^{13}\text{C}$  NMR data of **P1–P3** are more informative. The aromatic region of their  $^{13}\text{C}$  NMR spectra gives more precise information about the regiochemical structure of the main chain skeleton and reveals a high degree of structural regularity in the polymers. There are 16 well-resolved signals in the aromatic region in each case that correspond to the 16 aromatic carbons in the polymer structure. The six aliphatic signals are assigned to the long alkyl chains on the fluorene rings. In all cases,  $^{13}\text{C}$  NMR resonances arising from the quaternary carbon of the fluorene nucleus were clearly observed at around  $\delta$  55.4 ppm. The NMR spectral data supported the conclusion that these polymers have well-defined and symmetrical structures. The results are summarized in the Experimental Section.

**Molecular Weights and Thermal Properties.** The molecular weights of the polymers were measured by means of gel permeation chromatography (GPC) using THF as eluant against polystyrene standards. The results are listed in Table 1, and the degree of polymerization (DP) ranges from 13 to 21 repeat units per polymer chain. A similar molecular weight distribution was observed for an analogous copolymer consisting of the 2-ethylhexylcarbazole moiety.<sup>11</sup> The polydispersity indices  $M_w/M_n$  (1.3–1.5) are comparable to that observed (1.4) for the poly(9,9-dihexyl-2,7-fluorene) homopolymer (abbreviated as **PF-C<sub>6</sub>** in Chart 1).<sup>11</sup>

The thermal stability of the polymers was determined by thermogravimetric analysis (TGA) under nitrogen (Table 1). All of them exhibited an onset degradation temperature ( $T_d$ ) higher than 410 °C under nitrogen. **P3** has a slightly lower decomposition temperature than the other two. The degradation patterns for the three polymers are quite similar, with a main weight loss step at the onset temperature in the range of 410–440 °C. These data reveal that the polymers have excellent thermal stability and, in fact, are more thermally stable than the parent polymer **PF-C<sub>6</sub>** (decomposition onset  $T_d$  = 390 °C) and a related poly(fluorene-2-ethylhexylcarbazole) copolymer ( $T_d$  = 376 °C).<sup>11</sup> Thermally induced phase transition behavior of the polymers was also investigated with differential scanning calorimetry (DSC) in a nitrogen atmosphere. While PFs usually reveal a crystallization temperature due to their crystalline nature in the solid state, DSC curves of **P1–P3** showed no crystallization and melting peaks but only glass transition temperature ( $T_g$ ). This obviously indicates that the presence of the carbazole units in these copolymers effectively suppresses the crystallinity (or chain aggregation) of the polymer chains. All of our copolymers showed a  $T_g$  (170, 155, and 174 °C for **P1–P3**, respectively) higher than those of **PF-C<sub>6</sub>** (~103 °C)<sup>11</sup>

**Figure 1.** Photoluminescence (PL) spectra of **P1** (dotted line), **P2** (solid line), and **P3** (dashed line) in  $\text{CHCl}_3$  solutions at 293 K (Excitation wavelength = 340 nm, slit width = 0.3 nm).**Table 2. Photophysical Data of P1–P3 at 293 K**

polymer	$\text{CHCl}_3$ solution						film	
	$\lambda_{\text{abs}}$ (nm)	$\lambda_{\text{em}}$ (nm)	$\Phi_{\text{FI}}$	$\tau$ (ns)	$k_r$ ( $\text{s}^{-1}$ )	$k_{\text{nr}}$ ( $\text{s}^{-1}$ )	$\lambda_{\text{abs}}$ (nm)	$\lambda_{\text{em}}$ (nm)
<b>P1</b>	341	406	0.34	1.7	$2.0 \times 10^8$	$3.9 \times 10^8$	343, 368	426, 440
<b>P2</b>	341	405	0.47	1.9	$2.5 \times 10^8$	$2.8 \times 10^8$	347, 370	431
<b>P3</b>	343	404	0.33	2.1	$1.6 \times 10^8$	$3.2 \times 10^8$	344, 366	440

and other related *N*-alkylcarbazole-derived PF copolymers (79–113 °C).<sup>15,22</sup> This confirms the effect of the 9-arylcarbazole moiety in introducing disorder in the present system. The relatively high  $T_g$  values are essential for many applications, such as luminescent materials in OLEDs.

#### Absorption and Photoluminescence Properties.

The absorption and photoluminescence data were measured in both solution and solid state for **P1–P3**. The optical properties are summarized in Table 2. Each of them has an absorption maximum at around 341 nm that is almost invariant of the aryl substituent R. Likewise, the PL spectra of all the polymers in  $\text{CHCl}_3$  solutions are strikingly similar to each other, and they only show an emission peak at around 405 nm, irrespective of the identity of R (Figure 1). When the 9-arylcarbazole group was copolymerized into the polymer main chain in **P1–P3**, both the absorption and emission features are generally blue-shifted to shorter wavelengths, relative to the parent homopolymer **PF-C<sub>6</sub>** ( $\lambda_{\text{abs}}$  = 379 and  $\lambda_{\text{em}}$  = 415 nm in  $\text{CHCl}_3$ ).<sup>11</sup> This can be correlated to the fact that the 3,6-substitution of the carbazole decreases the conjugation by interrupting the linear  $\pi$ -system. The PL efficiencies ( $\Phi_{\text{FI}}$ ) of **P1–P3** were measured in their dilute  $\text{CHCl}_3$  solutions using quinine sulfate (0.1 N in  $\text{H}_2\text{SO}_4$ ) as a reference, and they showed decreased fluorescence quantum yields ( $\Phi_{\text{FI}}$  = 0.33–0.47) compared with **PF-C<sub>6</sub>** ( $\Phi_{\text{FI}}$  = 0.82) because of their shorter fluorene sequences. Apparently, the  $\Phi_{\text{FI}}$  value of **P2** appears to be larger than those of **P1** and **P3** presumably because of the higher degree of polymerization (DP = 21 in **P2**) with more fluorene rings in its polymer chain than the other two. All three polymers emitted blue light under UV excitation in the solid states. Both the solid-state absorption and PL spectra of **P1–P3** were slightly red-shifted with respect to their corresponding spectra in dilute solution, an indication that aggregation is not significant in the solid state (Figure 2). We also did not observe any strong concentration dependence of the absorption and fluorescence spectra for these polymers. To study the structural and conformational changes of the polymer in the film state,

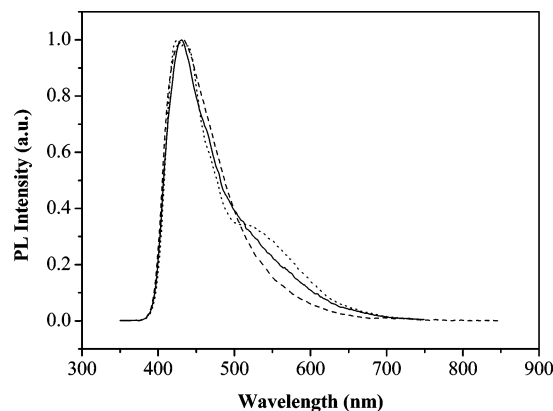


**Figure 2.** Solid-state thin-film PL spectra of **P1** (dotted line), **P2** (solid line), and **P3** (dashed line) at 293 K (Excitation wavelength = 325 nm, slit width = 0.2 mm).

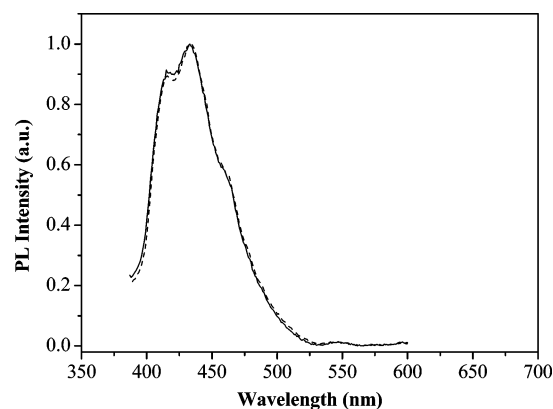


**Figure 3.** Solid-state thin-film PL spectra of **P3** before (solid line) and after (dashed line) annealing at 200 °C.

annealing experiments were performed on **P1–P3**. The film was spin-coated on a quartz substrate and then annealed at 200 °C (a temperature well above their  $T_g$ 's) in a vacuum oven for 24 h in air or under a nitrogen atmosphere. One striking property of these new copolymers was that no apparent change was observed for the absorption and PL spectra compared to the unannealed state in both conditions (Figure 3). This is in contrast to the previous work on PFs which showed that the PL spectrum of the annealed PF homopolymer film will typically suffer from a red shift in emission peak, and these undesirable spectral changes in PFs are attributed to the formation of low-energy excimer aggregates at high temperatures.<sup>10</sup> This suggests that **P1–P3** have a greater optical and luminescent stability than the purely polyfluorene homopolymer toward aggregation, and we think the interruption of the linearity of the polymer backbone by the alternate 3,6-carbazole units can hamper close chain packing. This observation is very similar to those reported by Advincula and Ding et al. for several random and alternating fluorene-based copolymers.<sup>15,22</sup>

The fluorescence decay parameters of the polymers in solution are also collected in Table 2. The PL emission maximum of the copolymers was monitored in each case. In dilute  $\text{CHCl}_3$  solution ( $10^{-5}$  M), the decay of the blue emission band for **P1–P3** was found to be single-exponential, with PL lifetimes ranging from 1.7 to 2.1 ns. Given the lack of interchain interactions in dilute solution, the observed emission associated with **P1–P3** is assigned to intrachain singlet excitons on the polymer backbones. As compared to the PF homopolymer ( $\tau =$

**Table 3. Band Gap Characteristics of P1–P3 As Determined from CV Data and Absorption Onset**

polymer	$E_{\text{ox}}$ (V) <sup>a</sup>	$E_{\text{red}}$ (V) <sup>b</sup>	$E_{\text{HOMO}}$ (eV) <sup>c</sup>	$E_{\text{LUMO}}$ (eV) <sup>c</sup>	$E_g$ (eV) <sup>d</sup>	$\lambda_{\text{abs}}(\text{onset})$ (nm)	$E_g$ (eV) <sup>e</sup>
<b>P1</b>	+0.64	−2.62	−5.04	−1.78	3.26	409	3.03
<b>P2</b>	+0.62	−2.60	−5.02	−1.80	3.22	406	3.05
<b>P3</b>	+0.65	−2.59	−5.05	−1.81	3.24	406	3.05

<sup>a</sup> Measured in  $\text{CH}_2\text{Cl}_2$  vs  $\text{Fc}/\text{Fc}^+$  couple. <sup>b</sup> Measured in THF vs  $\text{Fc}/\text{Fc}^+$  couple. <sup>c</sup> HOMO and LUMO levels were calculated by using the ferrocene value of 4.8 eV below the vacuum level. <sup>d</sup>  $E_g = \text{LUMO} - \text{HOMO}$ . <sup>e</sup>  $E_g$  estimated from the onset wavelength of the optical absorption.

0.52 ns),<sup>23</sup> the lifetime of the blue emission in the copolymers generally increases when the polyfluorene backbone is kinked by the carbazole linkage. Knowing the fluorescence quantum yields and the measured fluorescence lifetimes ( $\tau$ ) of **P1–P3**, the fluorescence radiative decay rate constant ( $k_r$ ) and nonradiative decay rate constant ( $k_{\text{nr}}$ ) at 293 K can be estimated using the expressions  $k_r = \Phi_{\text{F}}/\tau$  and  $k_{\text{nr}} = (1 - \Phi_{\text{F}})/\tau$ .<sup>24</sup> The estimated  $k_r$  and  $k_{\text{nr}}$  values at 293 K are  $(1.6\text{--}2.5) \times 10^8$  and  $(2.8\text{--}3.9) \times 10^8 \text{ s}^{-1}$  for **P1–P3**, and both the radiative and nonradiative rate constants reveal comparable orders of magnitude ( $10^8 \text{ s}^{-1}$ ).

**Electrochemical and Band Gap Studies.** Cyclic voltammetry (CV) was employed to evaluate the ionization potentials (i.e., hole-injection ability) and the redox stability of our copolymers. The CV curves were referenced to an Ag/AgCl reference electrode, which was calibrated using the ferrocene/ferrocenium ( $\text{Fc}/\text{Fc}^+$ ) redox couple. The oxidation and reduction potentials were used to determine the HOMO and LUMO energy levels which were calculated using the internal standard ferrocene value of −4.8 eV with respect to the vacuum level.<sup>25</sup> Hence, the highest occupied (HOMO) and lowest unoccupied (LUMO) molecular orbital energy levels of the copolymers can be estimated using the equations  $E_{\text{HOMO}} = -(E_{\text{ox}} + 4.8) \text{ eV}$  and  $E_{\text{LUMO}} = -(E_{\text{red}} + 4.8) \text{ eV}$ , respectively, where  $E_{\text{ox}}$  and  $E_{\text{red}}$  are the onset potentials for oxidation and reduction relative to the  $\text{Fc}/\text{Fc}^+$  couple. The results are gathered in Table 3. Polymers **P1–P3** showed similar CV curves in both p-doping and n-doping processes. The anodic sweeps were reversible and the oxidation waves occurred at potentials of +0.62 to +0.65 V for **P1–P3**. These oxidation potentials give  $E_{\text{HOMO}}$  values ranging from −5.02 to −5.05 eV for **P1–P3**. The cathodic wave was not observed in  $\text{CH}_2\text{Cl}_2$  solution from all of the polymers within the solvent limit. Attempts were then made to repeat the cathodic sweep in THF solution and a pseudo-reversible peak was located in the CV curve with the reduction potentials in the narrow range of −2.59 to −2.62 V. Accordingly, these values correspond to  $E_{\text{LUMO}}$  of −1.78 to −1.81 eV. These data revealed that polymers **P1–P3** with electron-rich carbazole units showed elevated HOMO energy levels relative to those of **PF-C6** (−5.50 eV) and other similar polyfluorene homopolymer, which means that **P1–P3** are more electropositive than the parent homopolymer, and we can expect a better hole-transporting ability in our copolymers. In fact, the hole injection from the ITO anode (work function = −4.8 eV) to **PF-C6** has a large energy barrier of ca. 0.70 eV. When half of the fluorene units was replaced by 9-arylcarbazole groups, the  $E_{\text{HOMO}}$  value of **P1–P3** was markedly raised to −5.02 to −5.05 eV relative to the vacuum level. This implies a significant lowering of the energy barrier to ca. 0.22–0.25 eV for injection from ITO using **P1–**

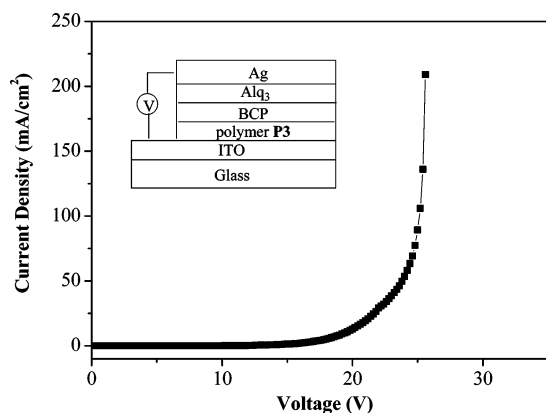


**Figure 4.** *I*–*V* characteristics of the PLED device ITO/P3/BCP/Alq<sub>3</sub>/Ag. The inset shows the PLED configuration.

**Table 4.** Electroluminescent Device Properties of P1–P3

polymer	EL $\lambda_{\text{em}}$ (nm)	$V_{\text{turn-on}}$ (V)	luminance (cd/m <sup>2</sup> )/ current efficiency (cd/A)/ current density (mA/cm <sup>2</sup> )	CIE coordinates	
				<i>x</i>	<i>y</i>
<b>P1</b>	445	15	30/0.03/219	0.221	0.242
<b>P2</b>	435	20	25/0.02/400	0.082	0.214
<b>P3</b>	444	15	40/0.02/209	0.201	0.218

**P3** as the active emissive layer. This has important implications on chemical tuning of the hole-transporting properties for these materials. Band gaps ( $E_g$ ) obtained experimentally were larger than those estimated from UV–vis data but follow the same trend, even though the UV–vis data do not account for exciton binding energy. This is probably caused by the interfacial energy barrier for charge injection.<sup>26</sup> It is also worthwhile to note that the redox behavior and the energy levels of the frontier orbitals do not seemingly change with the type of substituent R on the phenylene ring in **P1–P3**.

**Electroluminescent Properties.** We also studied the electroluminescent properties of our copolymers (Table 4). Although the incorporation of the carbazole unit can raise the HOMO energy levels, the LUMO levels of **P1–P3** are also raised, resulting in larger energy barriers for electron injection. As expected, the single-layer device of ITO/P3/Ag only gave a very weak EL emission with a brightness of 3 cd/cm<sup>2</sup>, even at a high current density of 520 mA/cm<sup>2</sup>. To improve the device performance, multilayer PLEDs of the configuration ITO/copolymer (90 nm)/BCP (25 nm)/Alq<sub>3</sub> (20 nm)/Ag (80 nm) were fabricated. All these multilayer devices exhibited typical electroluminescent diode behavior. The forward current was observed to increase superlinearly with the increase of applied voltage after exceeding the turn-on voltage (Figure 4). All the devices emitted almost pure blue light with a EL peak at 445, 435, and 444 nm for **P1–P3**, respectively, which matches well with the corresponding solid-state PL emission. This indicates that the same radiative excited states are involved in both EL and PL processes, and aggregate formation in the solid state is largely suppressed in the copolymers. A blue EL with negligible aggregate emission in the low-energy regime can be obtained from **P1–P3** by using BCP as a hole-blocking layer and Alq<sub>3</sub> as an electron-injection/transporting layer, and a representative EL spectrum is shown in Figure 5. This device structure can provide stable blue emission, and no voltage dependence of the EL spectra was observed. No emission from Alq<sub>3</sub> was observed from these devices, indicating that BCP can function as a hole-blocking material so that the holes can be confined in the polymer

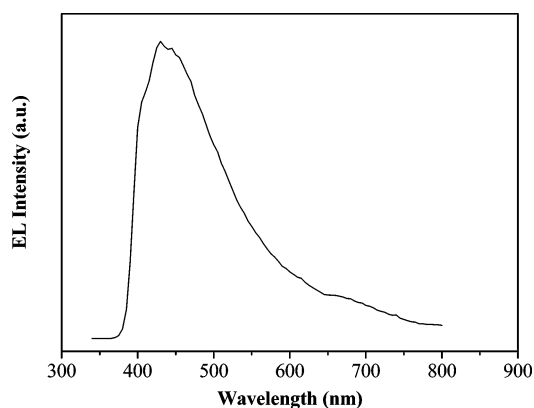


**Figure 5.** Representative EL spectrum of the PLED fabricated from **P2**.

layer to ensure that the electron–hole recombination only occurs in the polymer emissive layer. The CIE 1931 chromaticity coordinates of the PLEDs made from **P1–P3** are (0.221, 0.242), (0.082, 0.214), and (0.201, 0.218), respectively. The devices turned on at relatively high voltages ( $V_{\text{turn-on}} = 15$ –20 V), and the maximum luminance was 25–40 cd/m<sup>2</sup>. The high driving voltage was probably due to the silver cathode used in the devices and nonoptimized device structure and layer thickness. Even though the luminous efficiencies of the devices were not very high (ca. 0.02–0.03 cd/A), the external quantum efficiency was about 0.10% for diodes fabricated from **P1–P3**. Here, the device performance did not seem to vary significantly with the carbazolyl aryl substituent in the copolymers. These results show that nonradiative decay channels caused by aggregates can be avoided by such a copolymerization approach. We feel that there is still room for improvement when fabricating poly(fluorene–carbazole)-based PLEDs (e.g., by using other metal alloys as the cathode and/or addition of a hole-injection or -transporting layer between ITO and the polymer layer), and a detailed study of these LED devices is currently underway.

## Concluding Remarks

In this contribution, we have successfully copolymerized 9,9-dihexylfluorene and 9-arylcarbazole monomer units to produce three solution-processable alternating copolymers with well-defined chemical structures in good yields. All the copolymers were well characterized and exhibited good spectral properties both in solution and in film compared to the polyfluorene homopolymer. Efficient blue light emission, good solubility in common organic solvents, excellent thermal and luminescent stability, and high glass transition temperatures were all demonstrated with these kinked backbone structures, which render them promising candidates for use as the hole-transporting and light-emitting layer in stable blue PLEDs. Our new copolymers are stable blue light emitters, and the hole affinity has been improved. This study showed that the HOMO energy levels of PFs can be raised from around –5.50 to –5.02 eV by the addition of 9-arylcarbazole units to enhance the hole injection from the ITO anode. Incorporation of 3,6-carbazole “kink” linkages makes the parent PFs less prone to chain aggregation. Annealing of all copolymer films at 200 °C for 24 h resulted in no obvious changes in the absorption and emission spectra as compared with those of as-prepared films. This is probably due to the interruption of the linearity of the polymer backbone



by the 3,6-carbazole groups. Thus, the possibility of improved polyfluorene materials and luminescence properties through copolymerization with various carbazole partners has been illustrated. Incorporation of 9-aryl-carbazole group in the PF structure can provide a good route in improving the energy level mismatch between the anode and PFs. Future work will focus on improving device efficiency and lifetime by optimizing device structures.

**Acknowledgment.** W.-Y.W. thanks the Hong Kong Research Grants Council (Grant HKBU 2022/03P) and the Hong Kong Baptist University (FRG/01-02/II-48) for financial support. L.M.L. acknowledges the financial support from the Hong Kong Research Grants Council (Grant HKBU 2037/02P). We also thank Miss Suk-Yue Poon for her assistance on the electrochemical measurements.

**Supporting Information Available:** Preparations of 9-arylcarbazole derivatives, selected NMR spectra, absorption spectra, unannealed and annealed thin-film PL spectra, and other electroluminescent properties of the copolymers. This material is available free of charge via the Internet at <http://pubs.acs.org>.

## References and Notes

- Burroughes, J. H.; Bradley, D. D. C.; Brown, A. R.; Marks, R. N.; Mackay, K.; Friend, R. H.; Burn, P. L.; Holmes, A. B. *Nature (London)* **1990**, *347*, 539.
- (a) Friend, R. H.; Gymer, R. W.; Holmes, A. B.; Burroughes, J. H.; Marks, R. N.; Taliani, C.; Bradley, D. D. C.; Dos Santos, D. A.; Brédas, J. L.; Lögd Lund, M.; Salaneck, W. R. *Nature (London)* **1999**, *397*, 121. (b) Kraft, A.; Grimsdale, A. C.; Holmes, A. B. *Angew. Chem., Int. Ed.* **1998**, *37*, 402.
- (a) Shim, H. K.; Jin, J. I. *Adv. Polym. Sci.* **2002**, *158*, 193. (b) Segura, J. L. *Acta Polym.* **1998**, *49*, 319.
- (a) Kido, J.; Hongawa, K.; Okuyama, K.; Nagai, K. *Appl. Phys. Lett.* **1994**, *64*, 815. (b) McGehee, M. D.; Bergstedt, T.; Zhang, C.; Saab, A. P.; O'Regan, M. B.; Bazan, G. C.; Srdanov, V. I.; Heeger, A. J. *Adv. Mater.* **1999**, *11*, 1349. (c) Chen, F. C.; Yang, Y.; Thompson, M. E.; Kido, J. *Appl. Phys. Lett.* **2002**, *80*, 2308. (d) Swanson, S. A.; Wallraff, G. M.; Chen, J. P.; Zhang, W. J.; Bozano, L. D.; Carter, K. R.; Salem, J.; Villa, R.; Scott, J. C. *Chem. Mater.* **2003**, *15*, 2305.
- (a) Janietz, S.; Bradley, D. D. C.; Grell, M.; Giebeler, C.; Indasekaran, M.; Wu, W. W.; Woo, E. P. *Appl. Phys. Lett.* **1998**, *73*, 2453. (b) Kim, J. S.; Friend, R. H.; Cacialli, F. *Appl. Phys. Lett.* **1999**, *74*, 3084.
- (a) Neher, D. *Macromol. Rapid Commun.* **2001**, *22*, 1365. (b) Wong, W.-Y. *Coord. Chem. Rev.* **2005**, *249*, 971.
- (a) Tao, X.-T.; Zhang, Y.-D.; Wada, T.; Sasabe, H.; Suzuki, H.; Watanabe, T.; Miyata, S. *Adv. Mater.* **1998**, *10*, 226. (b) Kimoto, A.; Cho, J.-S.; Higuchi, M.; Yamamoto, K. *Macromolecules* **2004**, *37*, 5531. (c) Stephan, O.; Vial, J.-C. *Synth. Met.* **1999**, *106*, 115.
- (a) Cho, N. S.; Hwang, D.-H.; Lee, J.-I.; Jung, B.-J.; Shim, H.-K. *Macromolecules* **2002**, *35*, 1224. (b) Grell, M.; Long, X.; Bradley, D. D. C.; Inbasekaran, M.; Woo, E. P. *Adv. Mater.* **1997**, *9*, 798. (c) Leclerc, M. J. *Polym. Sci., Part A: Polym. Chem.* **2001**, *39*, 2867. (d) Liu, B.; Yu, W.-L.; Lai, Y.-H.; Huang, W. *Macromolecules* **2002**, *35*, 4975. (e) Wong, W.-Y.; Lu, G.-L.; Choi, K.-H.; Shi, J.-X. *Macromolecules* **2002**, *35*, 3506. (f) Wong, W.-Y.; Liu, L.; Shi, J.-X. *Angew. Chem. Int. Ed.* **2003**, *42*, 4064. (g) Wong, W.-Y.; Poon, S.-Y.; Lee, A. W.-M.; Shi, J.-X.; Cheah, K.-W. *Chem. Commun.* **2004**, 2420.
- (a) Lemmer, U.; Heun, S.; Mahrt, R. F.; Scherf, U.; Hopmeier, M.; Siegner, U.; Göbel, R. O.; Mullen, K.; Bassler, H. *Chem. Phys. Lett.* **1995**, *240*, 373. (b) Grüner, J.; Wittmann, H. F.; Hamer, P. J.; Friend, R. H.; Huber, J.; Scherf, U.; Müllen, K.; Moratti, S. C.; Holmes, A. B. *Synth. Met.* **1994**, *67*, 181. (c) Jenekhe, S. A.; Osaheni, J. A. *Science* **1994**, *265*, 765. (d) Kreyenschmidt, M.; Klaerner, G.; Fuhrer, T.; Ashenhurst, J.; Karg, S.; Chen, W. D.; Lee, V. Y.; Scott, J. C.; Miller, R. D. *Macromolecules* **1998**, *31*, 1099.
- (a) Bunz, U. H. F. *Chem. Rev.* **2000**, *100*, 1605 and references therein. (b) Bliznyuk, V. N.; Carter, S. A.; Scott, J. C.; Klärner, G.; Miller, R. D.; Miller, D. C. *Macromolecules* **1999**, *32*, 361. (c) Klärner, G.; Lee, J. I.; Lee, V. Y.; Chan, E.; Chen, J. P.; Nelson, A.; Markiewicz, D.; Siemens, R.; Scott, J. C.; Miller, R. D. *Chem. Mater.* **1999**, *11*, 1800. (d) Grell, M.; Bradley, D. D. C.; Long, X.; Chamberlain, T.; Inbasekaran, M.; Woo, E. P.; Soliman, M. *Acta Polym.* **1998**, *49*, 439. (e) Lee, J.-I.; Klärner, G.; Miller, R. D. *Chem. Mater.* **1999**, *11*, 1083.
- Liu, B.; Yu, W.-L.; Lai, Y.-H.; Huang, W. *Chem. Mater.* **2001**, *13*, 1984.
- (a) List, E. J. W.; Guentner, R.; Freitas, P. S.; Scherf, U. *Adv. Mater.* **2002**, *14*, 374. (b) Scherf, U.; List, E. J. W. *Adv. Mater.* **2002**, *14*, 477. (c) Gaal, M.; List, E. J. W.; Scherf, U. *Macromolecules* **2003**, *36*, 4236. (d) Gong, X.; Iyer, P. K.; Moses, D.; Bazan, G. C.; Heeger, A. J.; Xiao, S. S. *Adv. Funct. Mater.* **2003**, *13*, 325.
- Miteva, T.; Meisel, A.; Knoll, W.; Nothofer, H. G.; Scherf, U.; Müller, K.; Meerholz, K.; Yasuda, A.; Neher, D. *Adv. Mater.* **2001**, *13*, 565.
- (a) Fáber, R.; Stasko, A.; Nuyken, O. *Macromol. Chem. Phys.* **2000**, *201*, 2257. (b) Remmers, M.; Schulze, M.; Wegner, G. *Macromol. Rapid Commun.* **1996**, *17*, 239. (c) Martínez, A. G.; Barcina, J. O.; Cerezo, A. de F.; Schlüter, A.-D.; Frahn, J. *Adv. Mater.* **1999**, *1*, 27.
- Xia, C.; Advincula, R. C. *Macromolecules* **2001**, *34*, 5854.
- Donat-Bouillud, A.; Lévesque, I.; Tao, Y.; D'Iorio, M. *Chem. Mater.* **2000**, *12*, 1931.
- Ego, C.; Grimsdale, A. C.; Weil, T.; Enkelmann, V.; Müllen, K. *Adv. Mater.* **2002**, *14*, 809.
- Leclerc, M. J. *Polym. Sci., Part A: Polym. Chem.* **2001**, *22*, 1365.
- (a) Justin Thomas, K. R.; Lin, J. T.; Tao, Y.-T.; Ko, C.-W. *J. Am. Chem. Soc.* **2001**, *123*, 9404. (b) Justin Thomas, K. R.; Lin, J. T.; Tao, Y.-T.; Ko, C.-W. *Adv. Mater.* **2000**, *12*, 1949. (c) Zhu, Z.; Moore, J. S. *J. Org. Chem.* **2000**, *65*, 116. (d) Maruyama, S.; Tao, X.-T.; Hokari, H.; Noh, T.; Zhang, Y.; Wada, T.; Sasabe, H.; Watanabe, T.; Miyata, S. *J. Mater. Chem.* **1999**, *9*, 893. (e) Koene, B. E.; Loy, D. E.; Thompson, M. E. *Chem. Mater.* **1998**, *10*, 2235. (f) O'Brian, D. F.; Burrows, P. E.; Forrest, S. R.; Koene, B. E.; Loy, D. E.; Thompson, M. E. *Adv. Mater.* **1998**, *10*, 1108.
- (a) Yu, W. L.; Pei, J.; Cao, Y.; Huang, W.; Heeger, A. J. *Chem. Commun.* **1999**, 1837. (b) Liu, B.; Yu, W.-L.; Lai, Y.-H.; Huang, W. *Macromolecules* **2000**, *33*, 8945. (c) Schoo, H. F. M.; Demandt, R. C. J. E.; Vleggaar, J. J. M.; Liedenbaum, C. T. H. *Macromol. Symp.* **1997**, *125*, 165.
- (a) Hassan, J.; Sévignon, M.; Gozzi, C.; Schulz, E.; Lemaire, M. *Chem. Rev.* **2002**, *102*, 1359 and references therein. (b) Martínez-Palau, M.; Perea, E.; López-Calahorra, F.; Velasco, D. *Lett. Org. Chem.* **2004**, *1*, 231.
- (a) Lu, J.; Tao, Y.; D'Iorio, M.; Li, Y.; Ding, J.; Day, M. *Macromolecules* **2004**, *37*, 2442. (b) Li, Y.; Ding, J.; Day, M.; Tao, Y.; Lu, J.; D'Iorio, M. *Chem. Mater.* **2004**, *16*, 2165.
- Teetsov, J.; Fox, M. A. *J. Mater. Chem.* **1999**, *9*, 2117.
- (a) Turro, N. J. *Modern Molecular Photochemistry*; University Science Books: Mill Valley, CA, 1991. (b) Samuel, I. D. W.; Rumbles, G.; Collison, C. J. *Phys. Rev. B* **1995**, *52*, 11573.
- Thelakkat, M.; Schmidt, H.-W. *Adv. Mater.* **1998**, *10*, 219.
- Chen, Z. K.; Huang, W.; Wang, L. H.; Kang, E. T.; Chen, B. J.; Lee, C. S.; Lee, S. T. *Macromolecules* **2000**, *33*, 9015.

MA050693+